

Semiconductive 3-D Haloplumbate Framework Hybrids with High Color Rendering Index White-Light Emission

Guan-E Wang, Gang Xu,* Ming-Sheng Wang, Li-Zhen Cai, Wen-Hua Li, Guo-Cong Guo*

State Key Laboratory of Structural Chemistry, Fujian Institute of Research on the Structure of Matter, Chinese Academy of Sciences, Fuzhou, Fujian 350002, P. R. China.

E-mail: gxu@fjirsm.ac.cn; gcguo@fjirsm.ac.cn

EXPERIMENTAL SECTION

Materials and Instruments. All reagents were purchased commercially and used without further purification. Elemental analyses of C, H, and N were performed on an Elementar Vario EL III microanalyzer. Powder X-ray diffraction (PXRD) patterns were recorded on a Rigaku MiniFlex II diffractometer using Cu $K\alpha$ radiation. Optical diffuse reflectance spectra were measured at room temperature with a Perkin-Elmer Lambda 900 UV-Vis spectrophotometer. The instrument was equipped with an integrating sphere and controlled by a personal computer. The samples were ground into fine powder and pressed onto a thin glass slide holder. The BaSO₄ plate was used as a standard (100% reflectance). The absorption spectra were calculated from reflectance spectra using the Kubelka-Munk function: $\alpha/S = (1-R)^2/2R$, where α is the absorption coefficient, S is the scattering coefficient (which is practically wavelength independent when the particle size is larger than 5 μm), and R is the reflectance. Solid-state photoluminescent excitation, emission spectra were performed on an Edinburgh EI920 fluorescence spectrometer equipped with a 450-W Xe lamp and a R928P PMT detector. The lifetimes of **1** and **2** were also measured on an Edinburgh EI920 fluorescence spectrometer equipped with nF900 lamp and a R928P PMT detector. The quantum yield was measured on an Edinburgh FLS920 fluorescence spectrometer equipped with a BaSO₄-coated integrating sphere, a 450 W Xe lamp, and a R928P PMT detector in the single-photon counting mode. The test condition is the same, including excitation slit and emission slit width, dwell time, repeats number, filter, excitation wavelength, and the same sample holder with a $0.3 \times 1 \text{ cm}^2$. The CIE coordinates, CRI and CCT were calculated using

the CIE calculator-version 3 software. The direct current (DC) I-V analysis was measured on KEITHLEY4200-SCS. Gold wires (50 μm ϕ) were attached to the electrodes on the substrate by gold paste. A NETZSCH STA 449C thermogravimetric analyzer was used to obtain thermogravimetry (TG) curves in N_2 with a flow rate of 20 mL min^{-1} and a ramp rate of 10 $^\circ\text{C min}^{-1}$ in the temperature range of 30–900 $^\circ\text{C}$.

Syntheses of 1 and 2. A mixture of PbCl_2 (**1**: 1.3 mmol, 0.365 g; **2**: 1.0 mmol, 0.278 g), DABCO (0.5 mmol, 0.056 g), alcohols (4 mL; *N*-butanol for **1**, ethanol for **2**), and concentrated HCl (2.0 mL, 36%) was heated at 170 $^\circ\text{C}$ for 5 days in a sealed 25-mL Teflon-lined stainless steel vessel. Upon cooling at 3 $^\circ\text{C h}^{-1}$ to room temperature, colorless crystals were gained, yield: 85% for **1** and 90% for **2**. Both compounds are stable in air. The phase purity of **1** and **2** were verified by elemental analysis and PXRD determination (Fig. S1). Elem. Anal. (%): Compound **1**: Calcd.: C, 9.72; H, 1.89; N, 3.78. Found: C, 9.78; H, 1.91; N, 3.83; Compound **2**: Calcd.: C, 12.28; H, 2.29; N, 2.86. Found: C, 12.38; H, 2.45; N, 2.91. CCDC: 1055380 for **1**, 1055381 for **2**.

Syntheses of $\text{H}_2(\text{DABCO})\text{Cl}_2$ and $[\text{Et}_2\text{DABCO}]\text{I}_2$. 2 mL of HCl solution were carefully dropped to a water solution of DABCO (224 mg, 2 mmol). The solution was heated under reflux for 2 h and put into a dryer with anhydrous silica gel. The colorless block crystals of $\text{H}_2\text{DABCOCl}_2$ were obtained after 3 days of slow evaporation. $[\text{Et}_2\text{DABCO}]\text{I}_2$ was obtained by the same method but using iodoethane instead of HCl.

Single-Crystal Structure Determination. The intensity data sets were collected on a Rigaku Saturn 70 CCD diffractometer for **1** and a Rigaku MM007-Saturn 724 diffractometer for **2**, equipped with graphite-monochromated Mo $K\alpha$ radiation ($\lambda = 0.71073 \text{ \AA}$) using the ω -scan technique at 293 K. The data sets were reduced with the CrystalClear program. An empirical absorption correction was applied using the multi-scan method. The structures were solved by direct methods using the Siemens SHELXL package of crystallographic software. The difference Fourier maps were created on the basis of these atomic positions to yield the other non-hydrogen atoms. The structures were refined using a full-matrix least-squares refinement on F^2 . All non-hydrogen atoms were refined anisotropically. The hydrogen atoms of DABCO molecules were added geometrically and refined using the riding model.

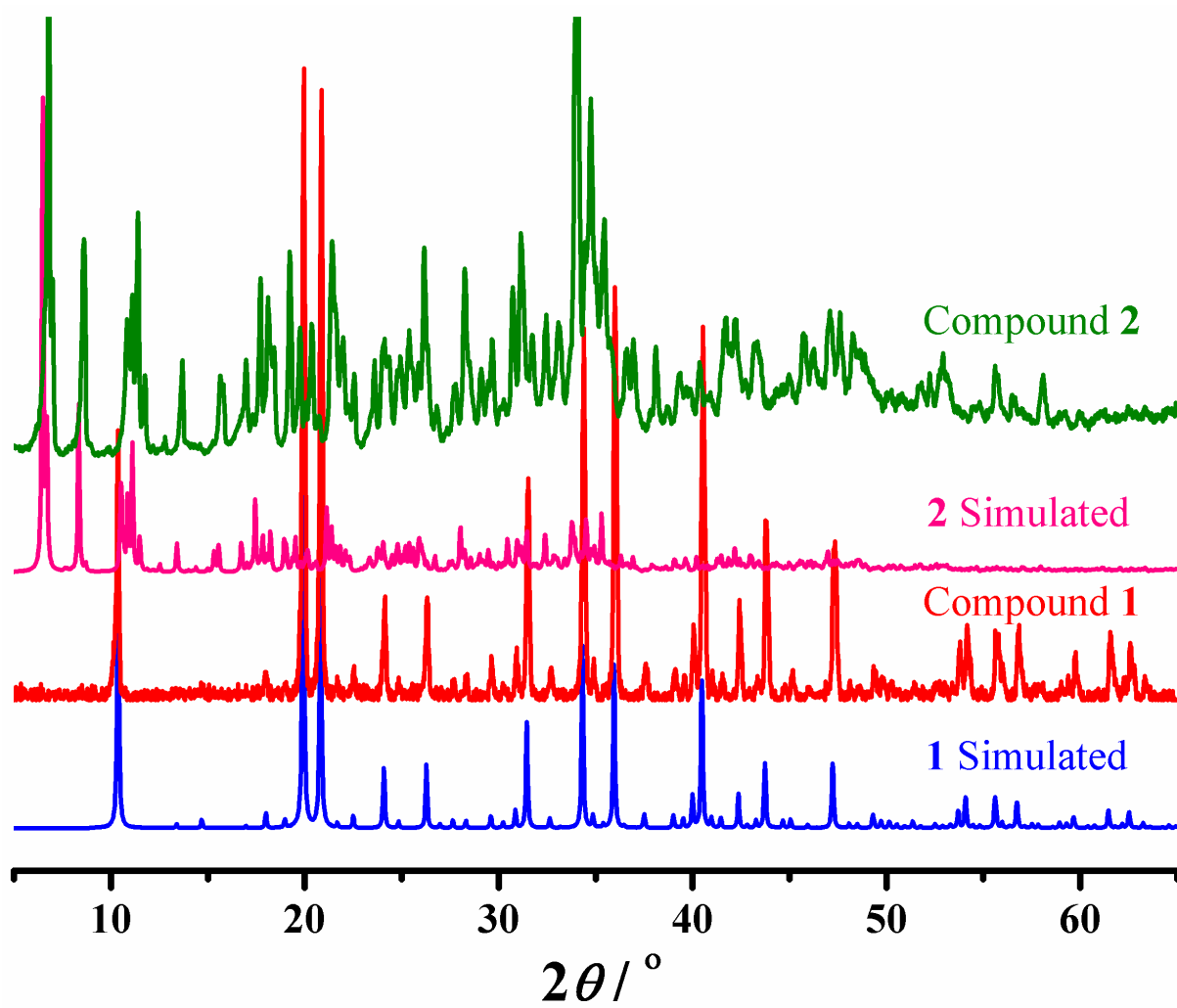


Fig. S1. PXRD patterns of compounds 1 and 2.

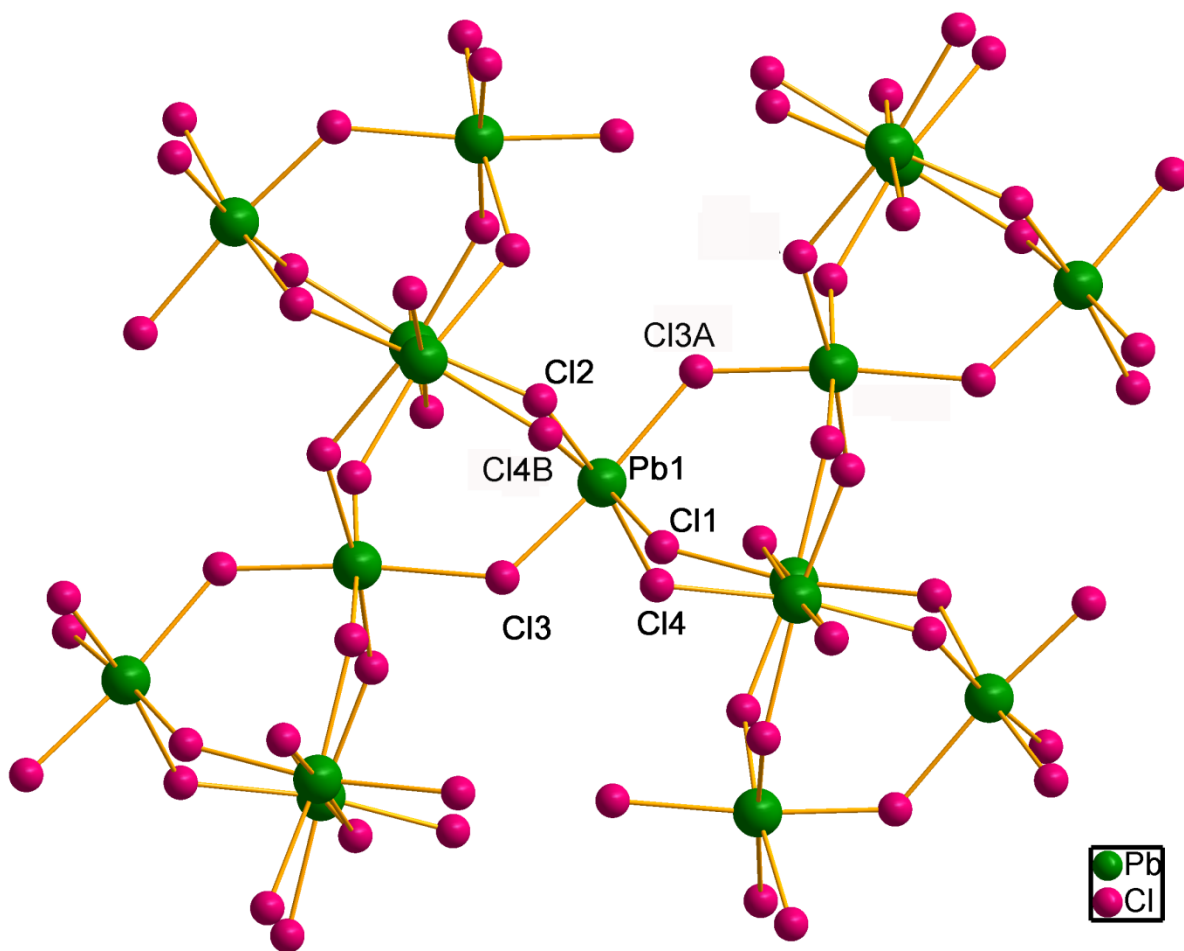


Fig. S2. Coordination environment of Pb in compound 1. Symmetric code: A: $0.5+x, 2.5-y, -0.75-z$; B: $1.5-y, 1.5+x, -0.25+z$.

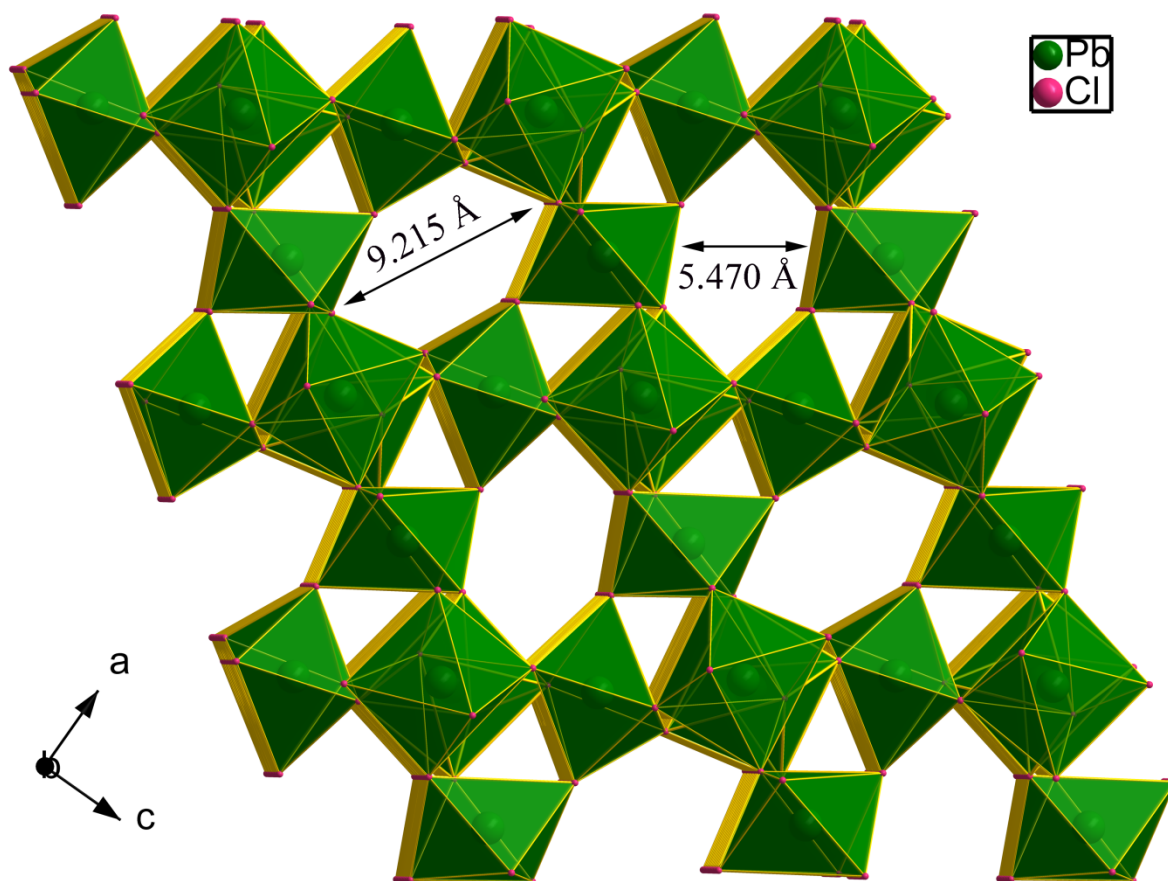


Fig. S3. Structure of the $(\text{Pb}_2\text{Cl}_6)^{2-}$ framework viewed along the b axis in compound **1**. Coordination spheres of Pb(II) atoms are shown as polyhedra for clarity.

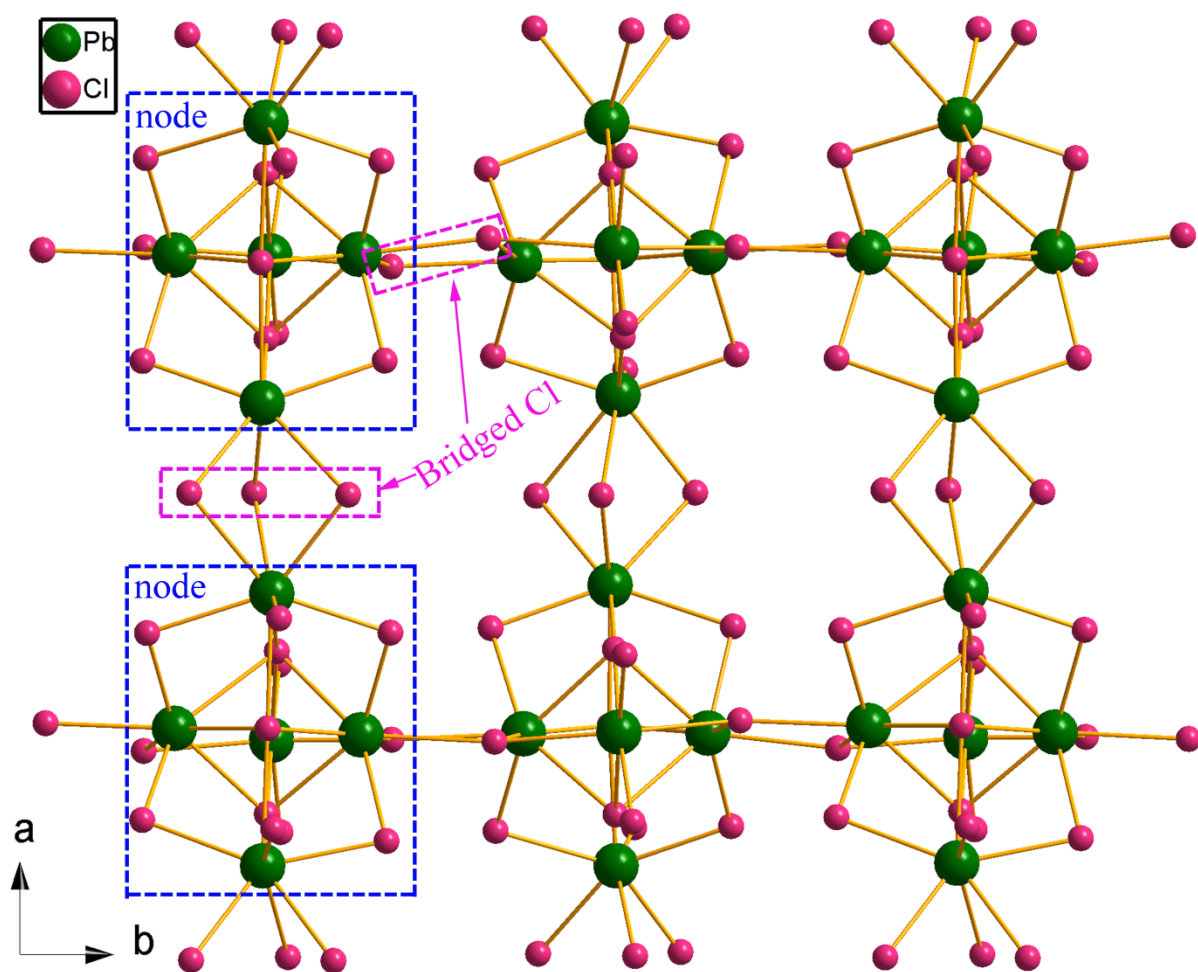


Fig. S4. Topological node of the trigonal bipyramid shaped $\text{Pb}_5\text{Cl}_{18}$ cluster in compound **2**.

The three Cl bridged atoms are Cl16–Cl18, and the two bridged atoms are Cl11–Cl12.

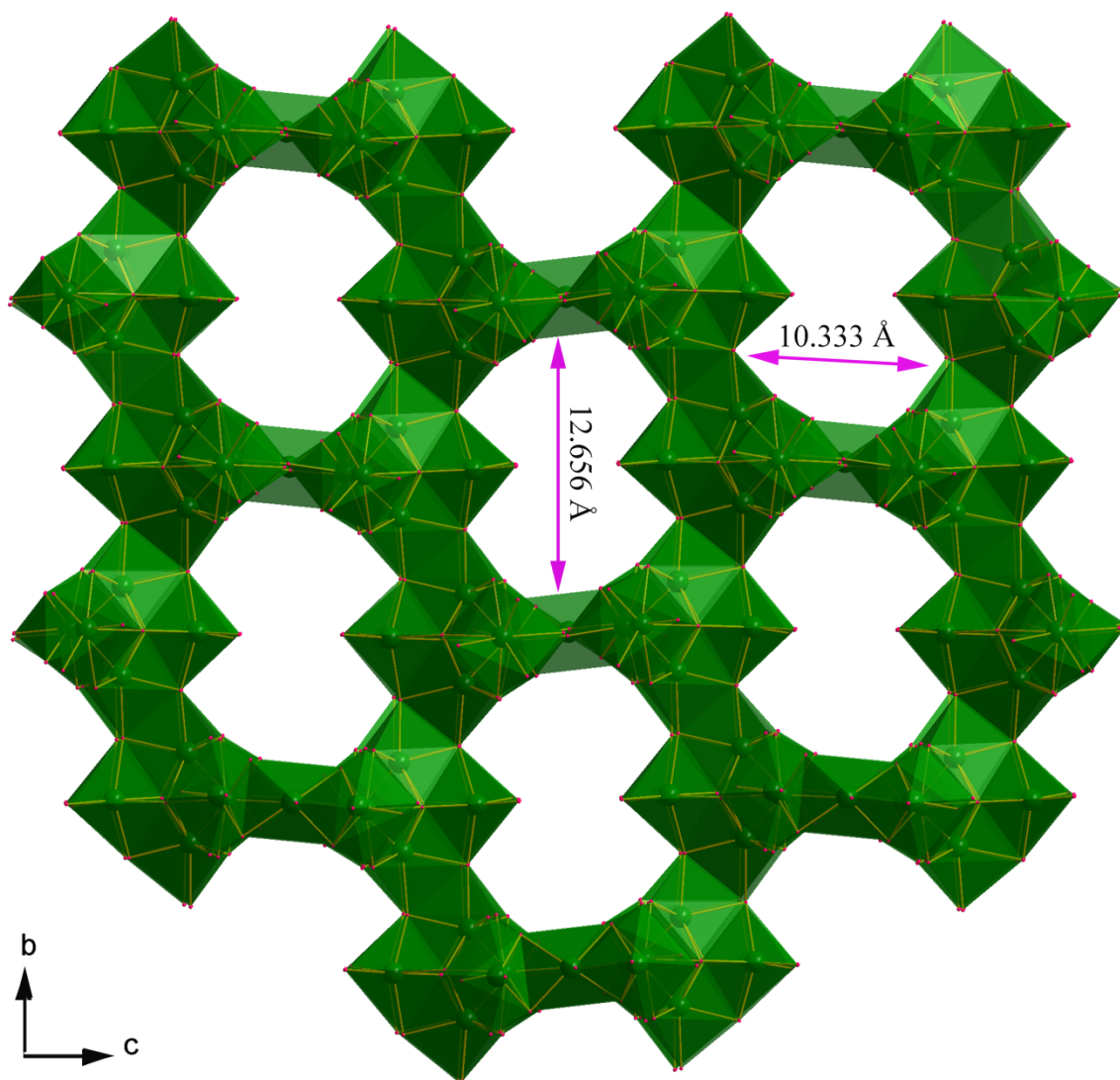


Fig. S5. Structure of the $(\text{Pb}_{21}\text{Cl}_{59}^{17-})$ framework viewed along *a* axis in compound **2**. Coordination spheres of Pb(II) atoms are shown as polyhedra for clarity.

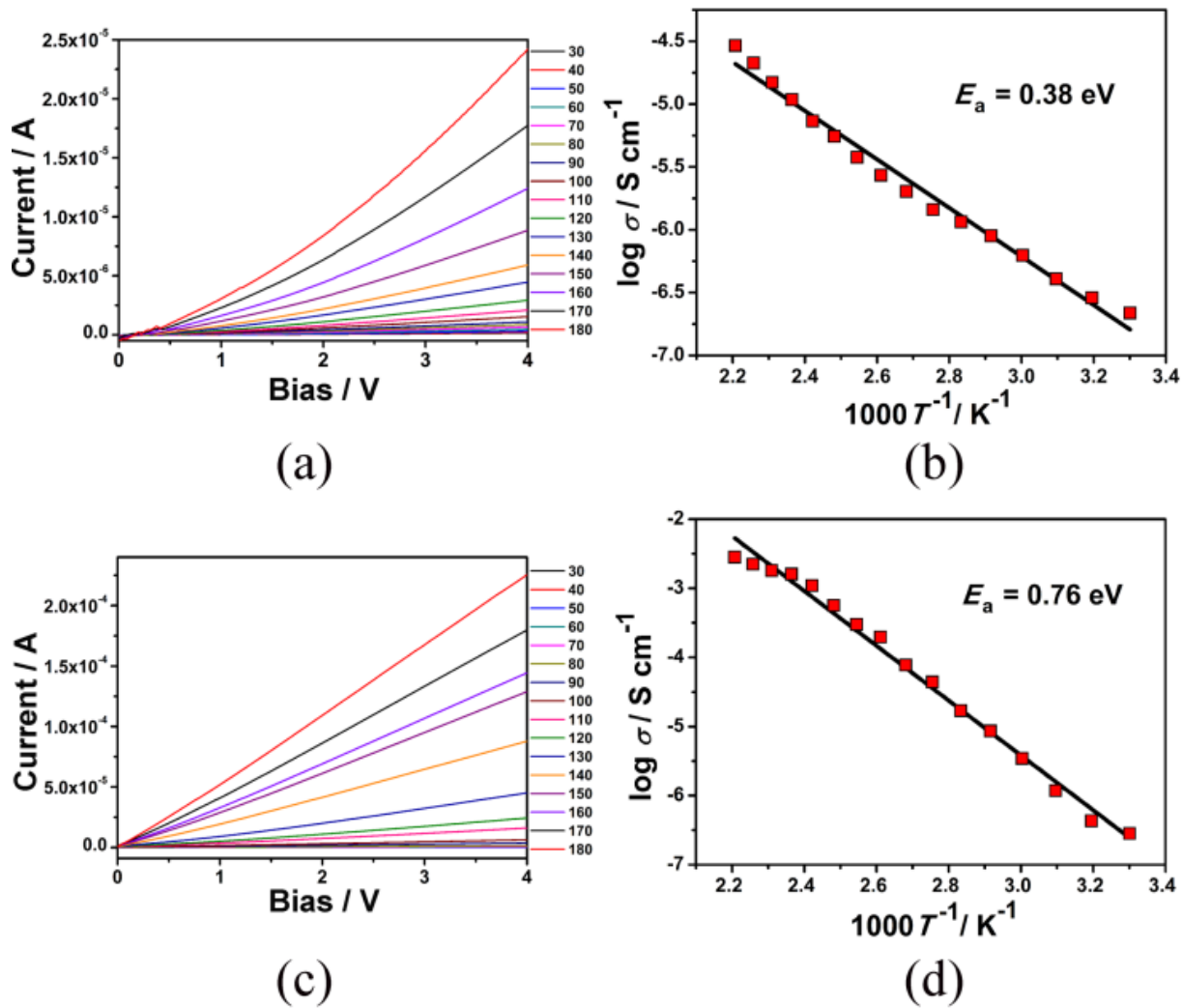


Fig. S6. Temperature-dependent I–V curves and Arrhenius plots for **1** (a, b) and **2** (c, d). E_a is the activation energy.

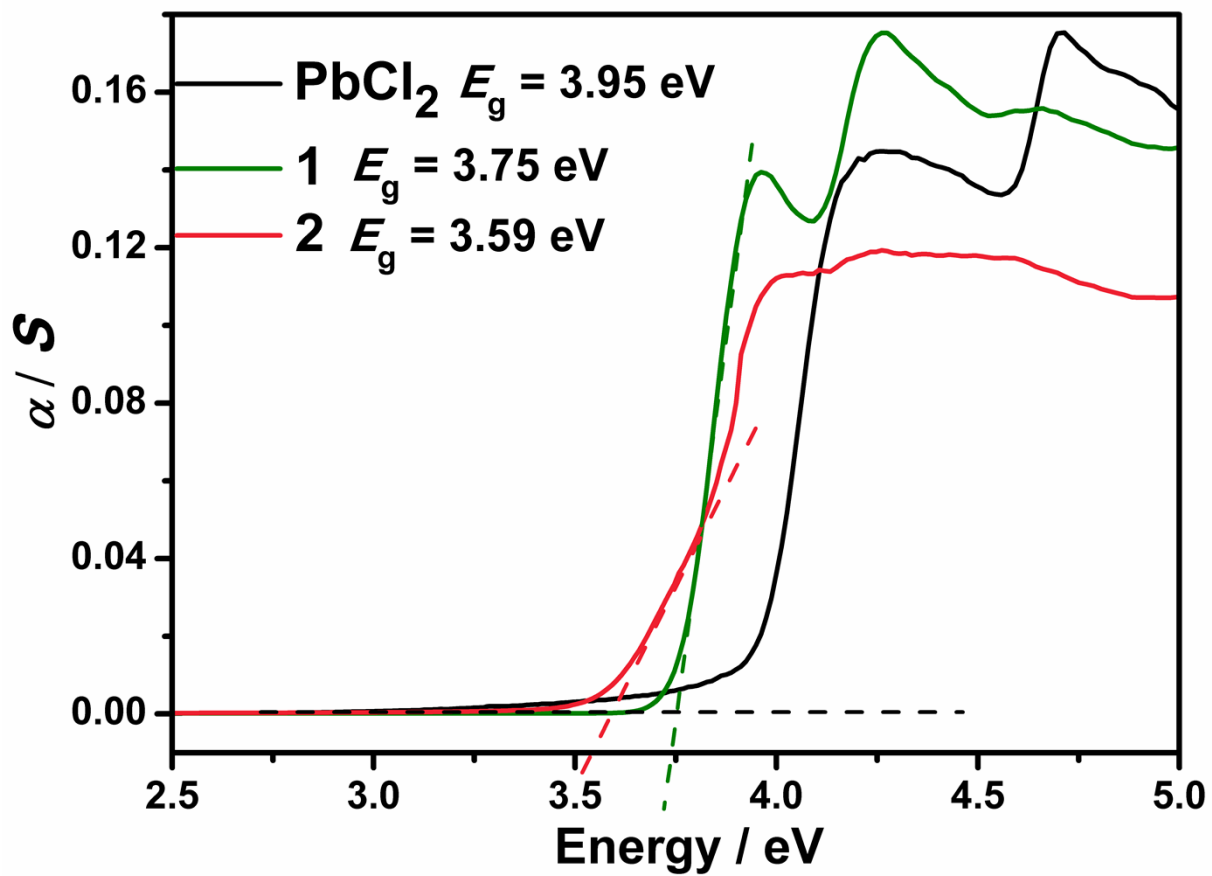


Fig. S7. Optical absorption spectra for 1, 2, and PbCl_2 .

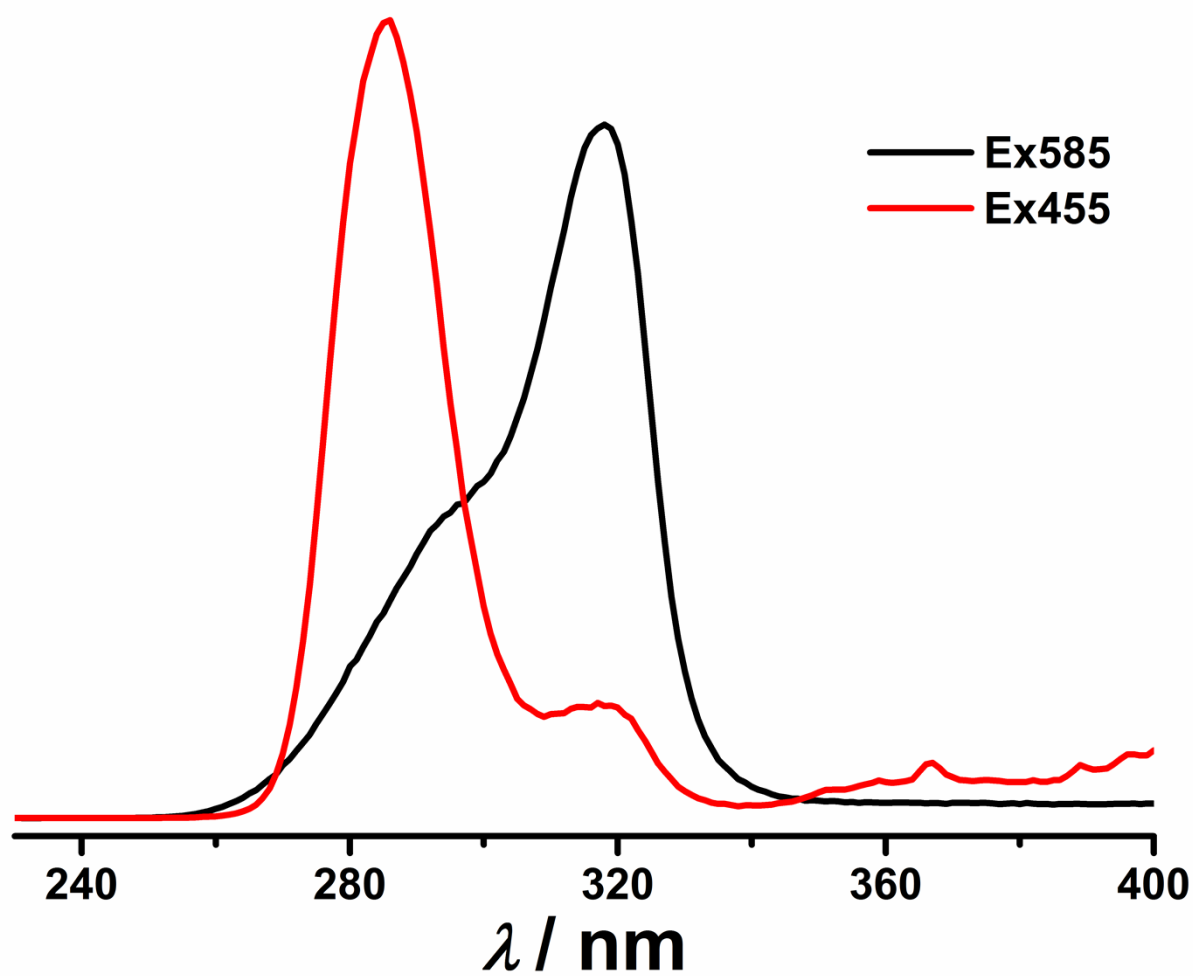
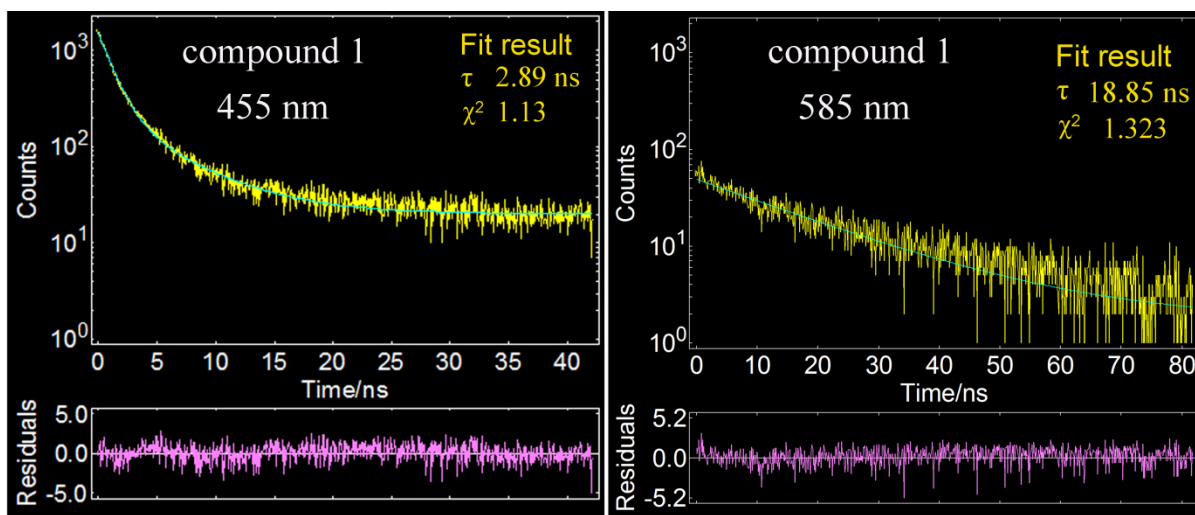
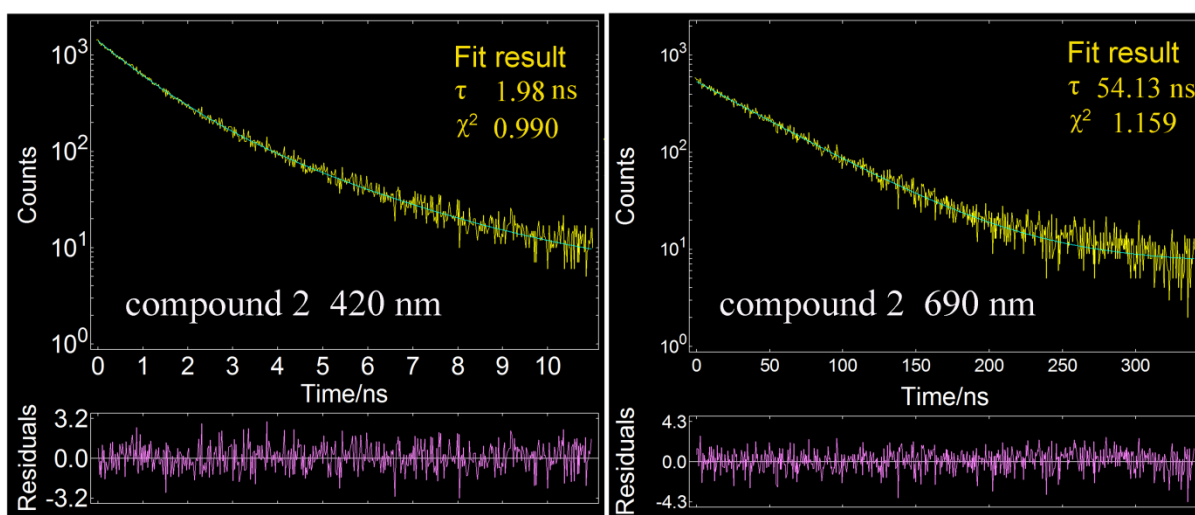


Fig. S8. Excitation spectra of compound 1.



(a)

(b)



(c)

(d)

Fig. S9. Phosphorescence decay data and the fitting curve of **1** at 455 nm (a), 585 nm (b) emission, and compound **2** at 420 nm (c), 690 nm (d) emission.

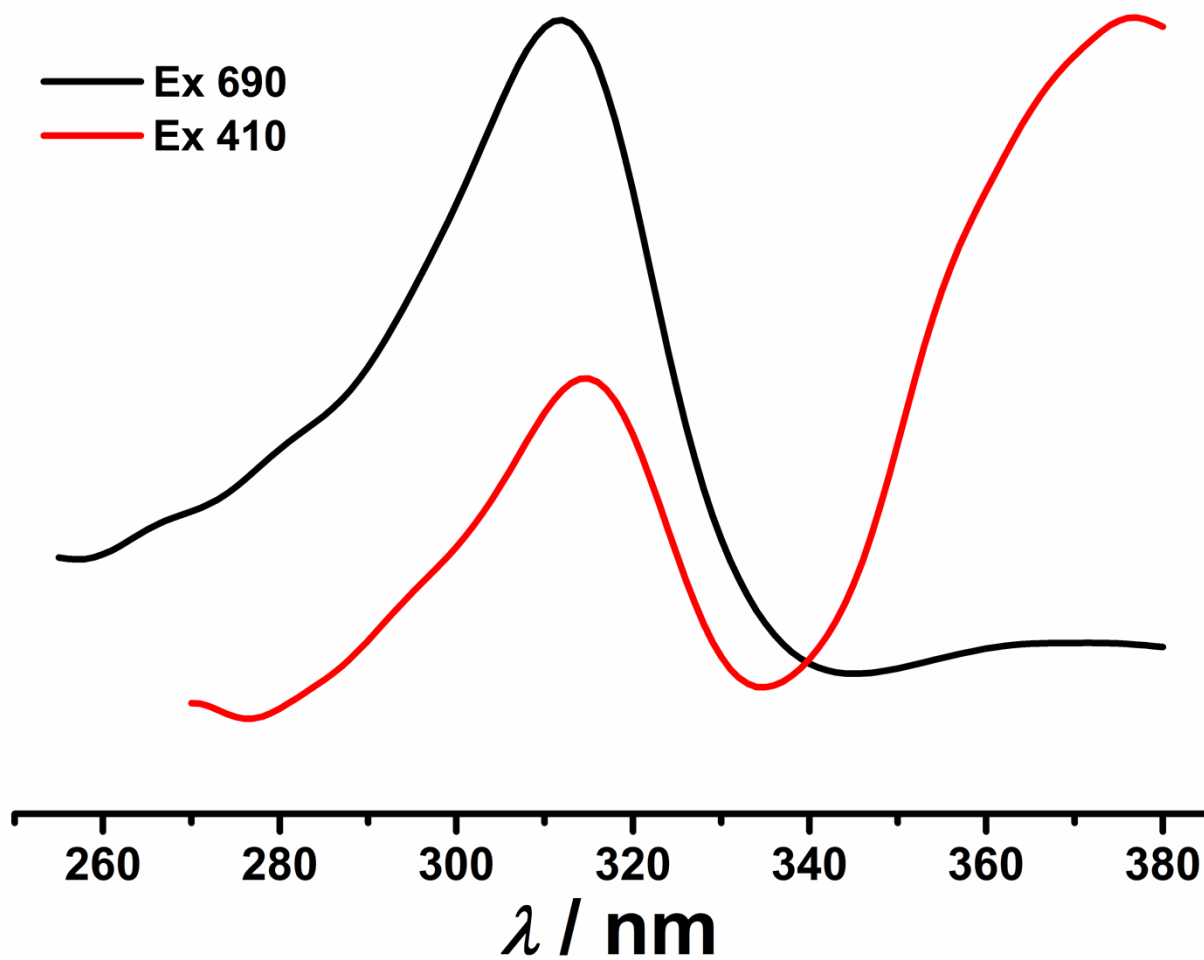


Fig. S10. Excitation spectra of compound 2.

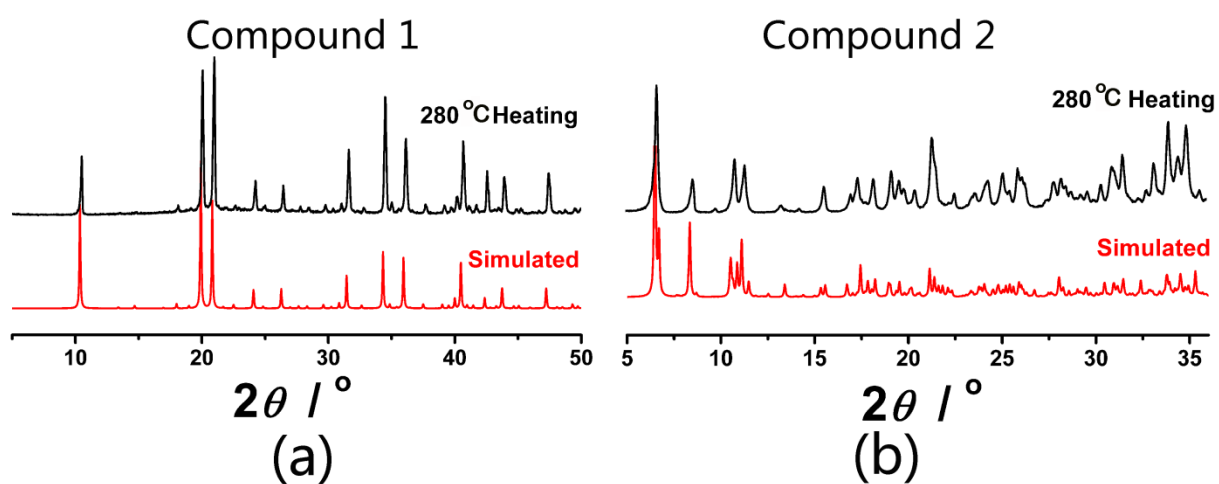


Fig. S11. PXRD patterns of 1 and 2 after annealing to 280 °C for 2 hours.

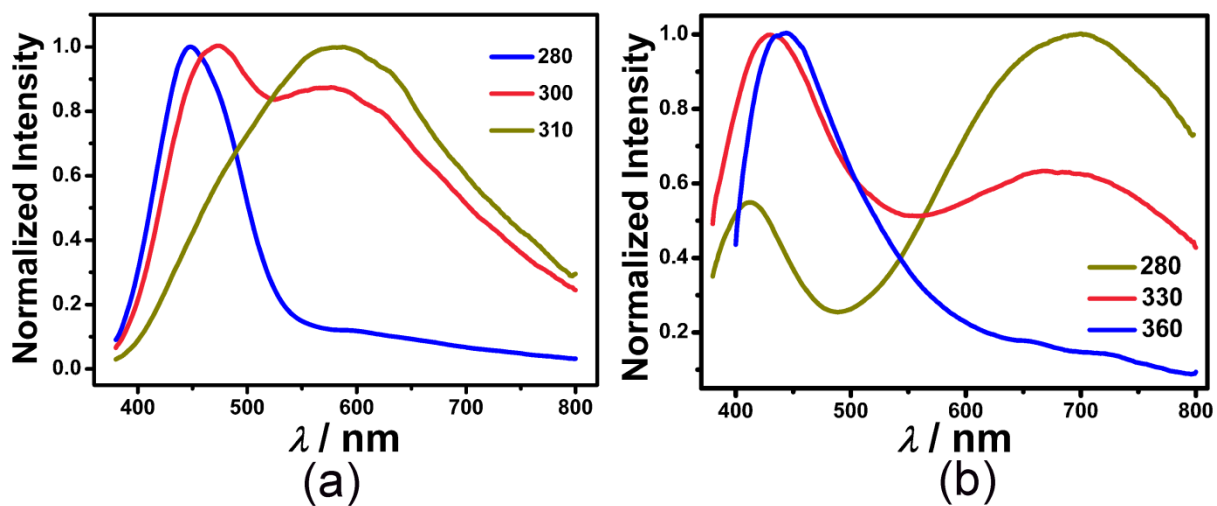


Fig. S12. Solid-state photoluminescent spectra of 1 (a) and 2 (b) by variation of excitation light after annealing at 280 °C for 2 hours.

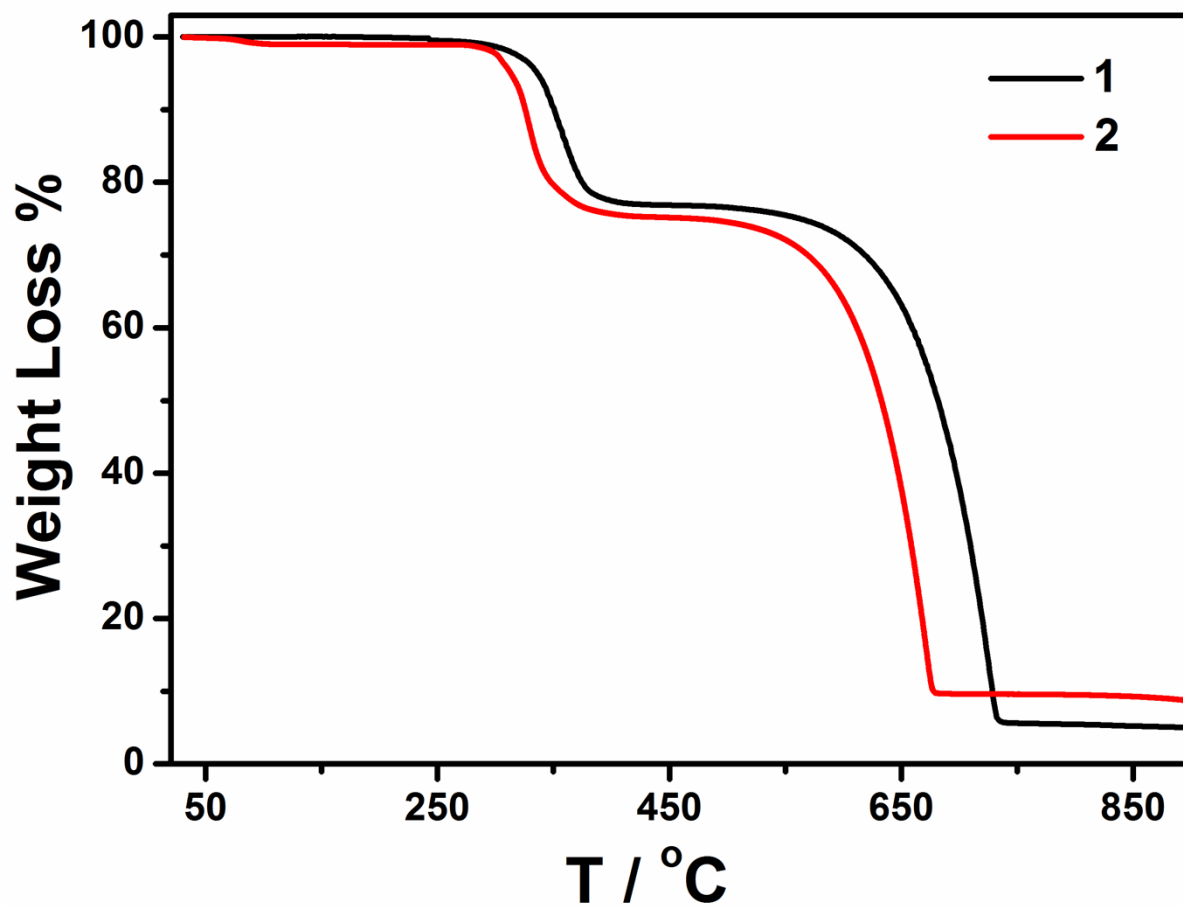


Fig. S13. TG curves of compounds 1 and 2.

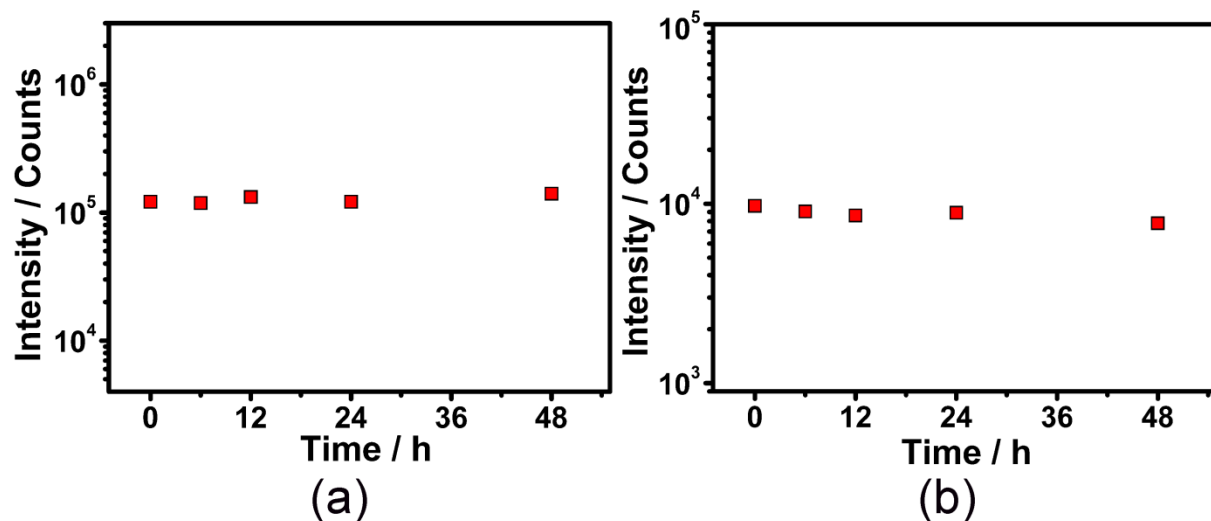


Fig. S14. The intensity of the white light emission at 455 nm for 1 (a) and 420 nm for 2 (b).

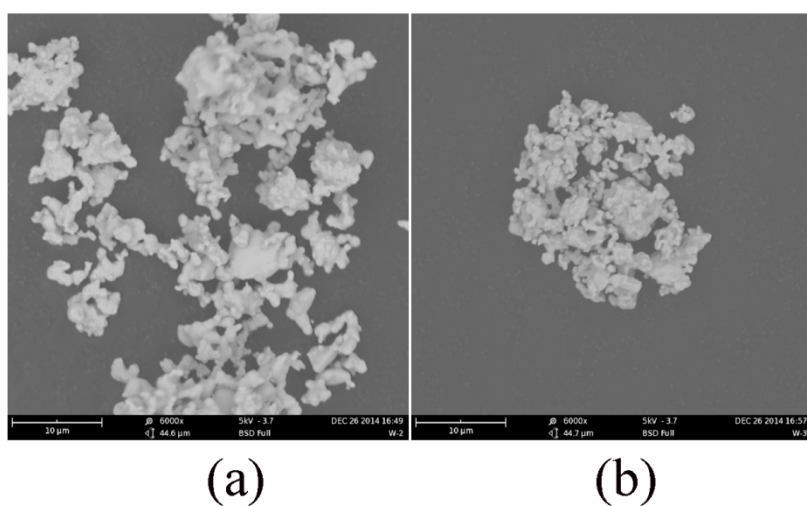


Fig. S15. SEM images of ball-milled powders of (a) 1, (b) 2.

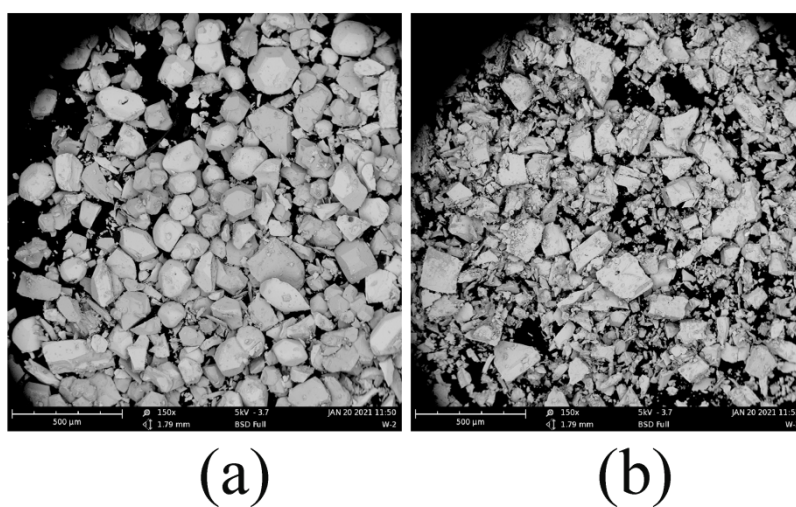


Fig. S16. SEM images of hand-milled powders of (a) 1, (b) 2.

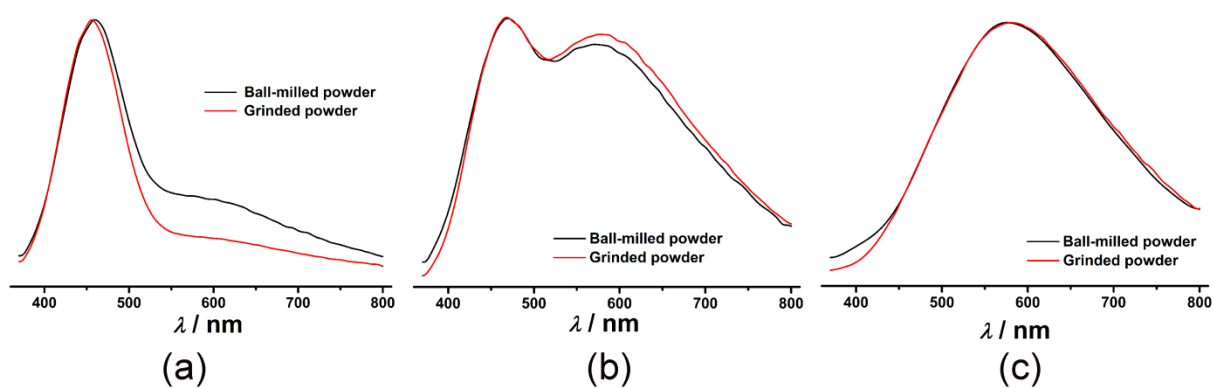


Fig. S17. Photoluminescence of compound **1** from hand grinded powder and ball-milled powders excited at (a) 280 nm, (b) 300 nm, and (c) 310 nm, respectively.

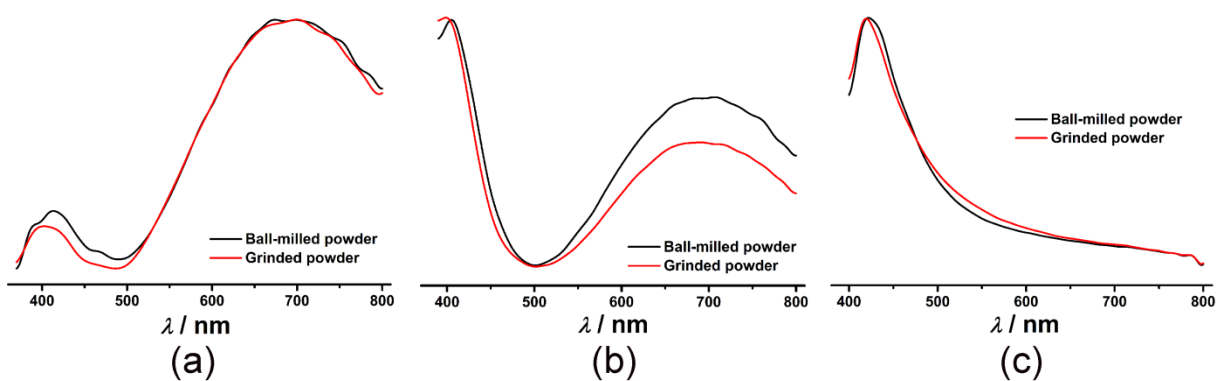


Fig. S18. Photoluminescence of compound **2** from hand grinded powder and ball-milled powders excited at (a) 280 nm, (b) 330 nm, and (c) 360 nm, respectively. Because the emission of the sample were not done at the same time, there is a little difference between the ball-milled powder and grinded powder.

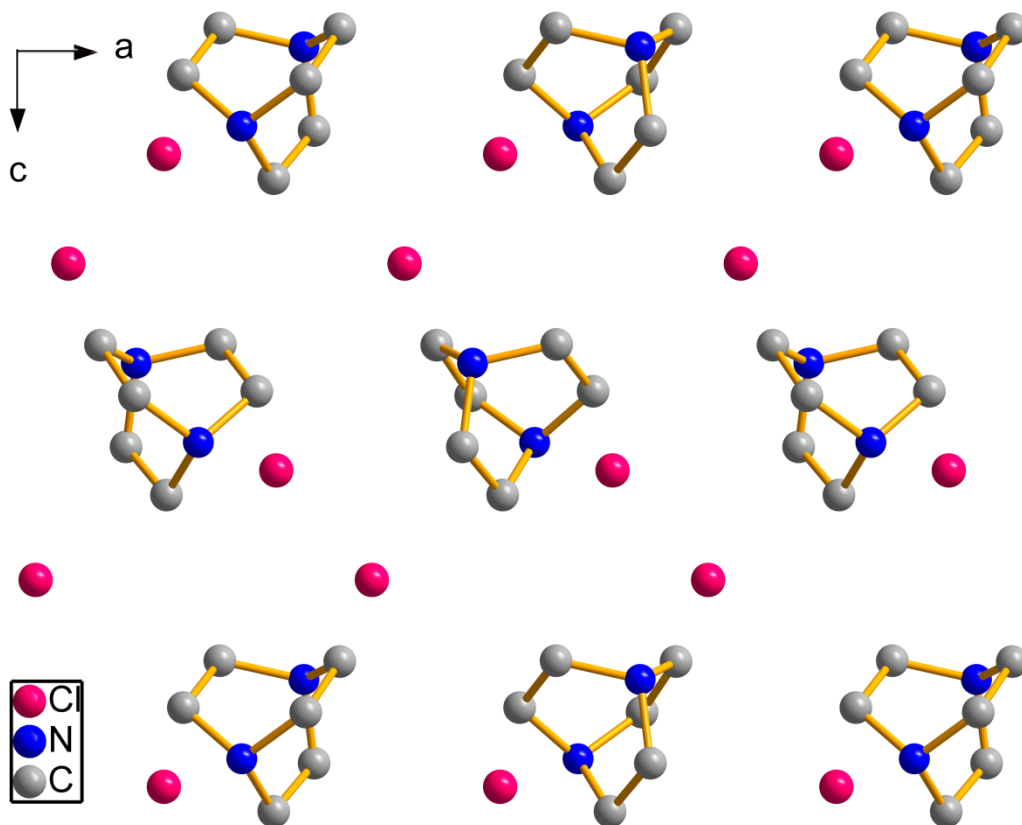


Fig. S19. Crystal structure of $\text{H}_2(\text{DABCO})\text{Cl}_2$ viewed along the b direction. Hydrogen atoms are omitted for clarity.

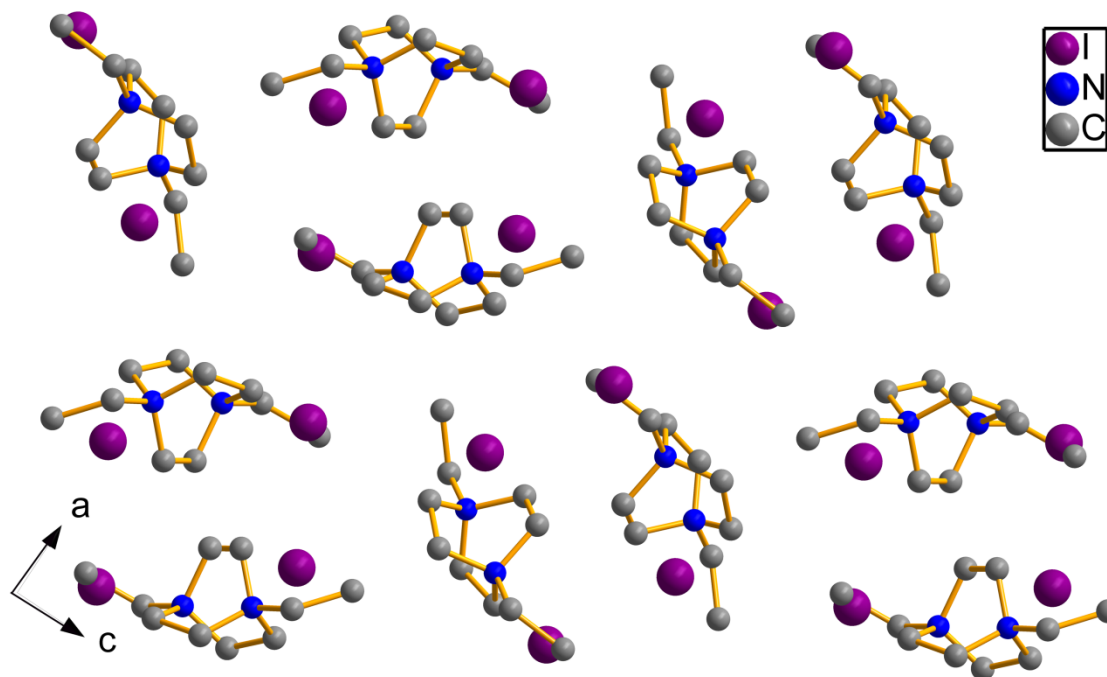


Fig. S20. Crystal structure of $[\text{Et}_2\text{DABCO}]\text{I}_2$ viewed along the b direction. Hydrogen atoms are omitted for clarity.

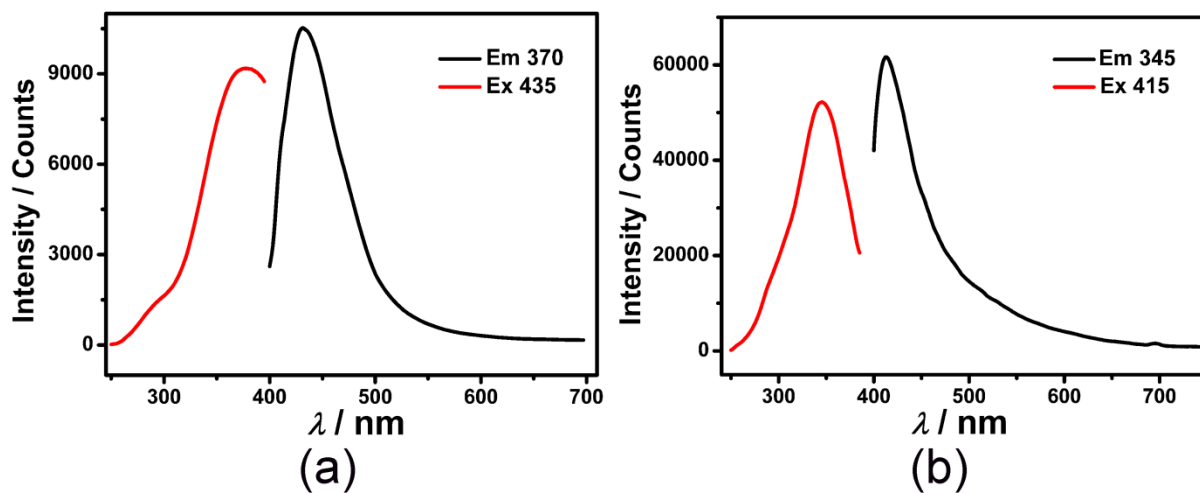


Fig. S21. (a) Emission and excitation spectra of $\text{H}_2(\text{DABCO})\text{Cl}_2$. (b) Emission and excitation spectra of $[\text{Et}_2\text{DABCO}]\text{I}_2$.

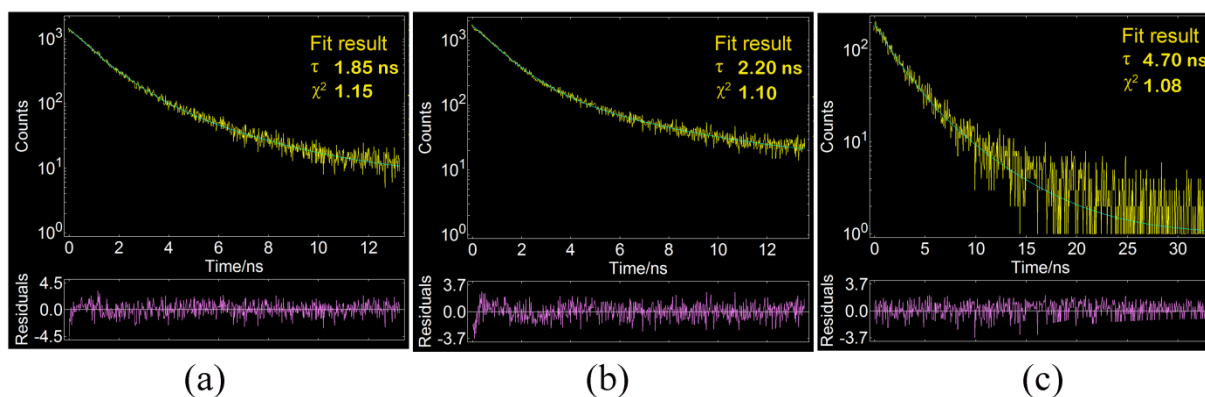


Fig. S22. Phosphorescence decay data and the fitting curve of $\text{H}_2(\text{DABCO})\text{Cl}_2$ at 435 nm emission (a), $[\text{Et}_2\text{DABCO}]\text{I}_2$ at 415 nm emission (b), and PbCl_2 at 545 nm emission (c).

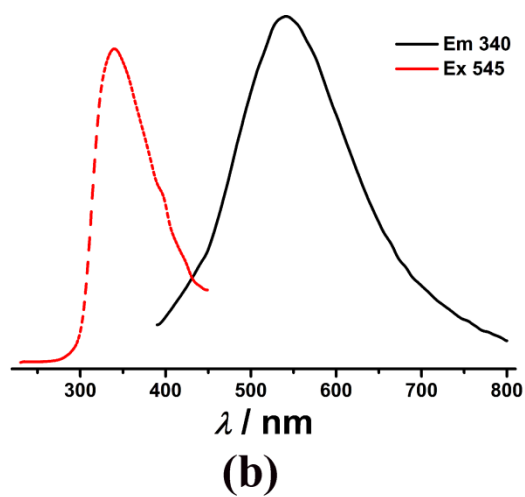


Fig. S23. Emission spectrum of PbCl_2 excited at a wavelength of 340 nm, and the excitation spectrum of PbCl_2 at 545 nm.

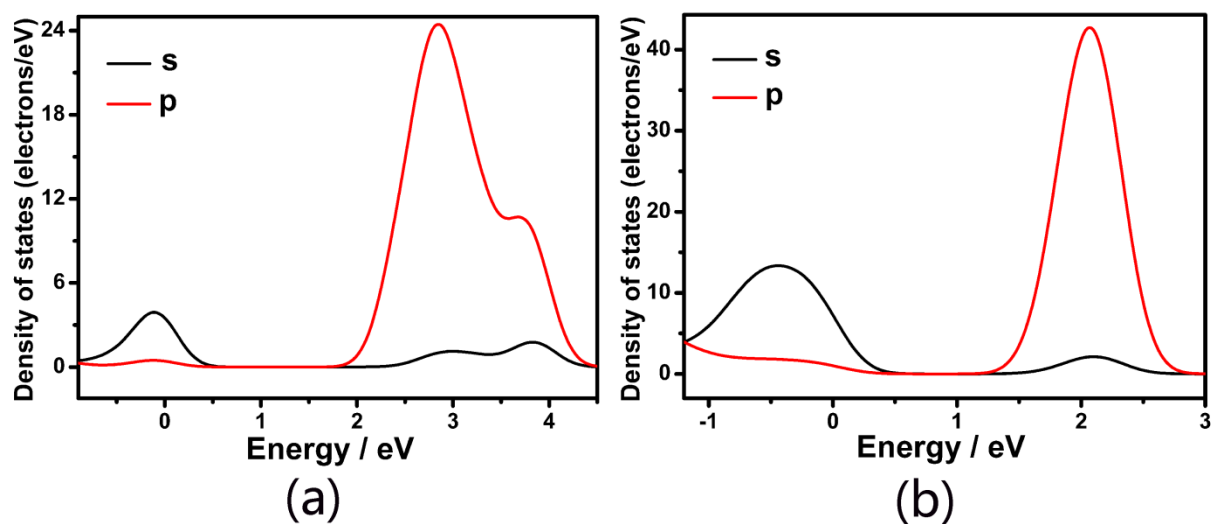


Fig. S24. The density of states of Pb^{2+} ion in compound **1** (a) and **2** (b).

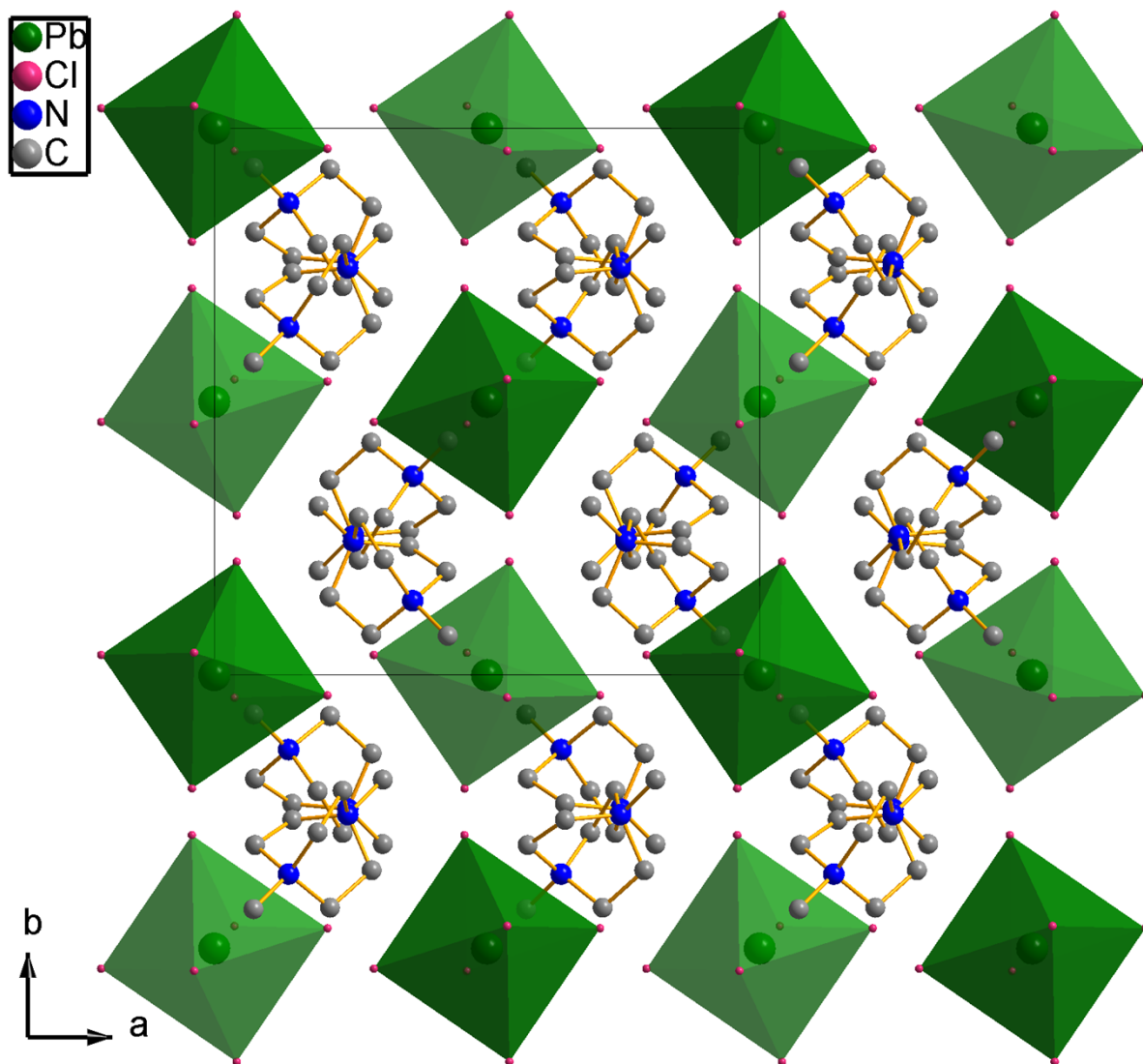


Fig. S25. The crystal structure of $(\text{Me}_2\text{DABCO})_2(\text{PbCl}_6)$.

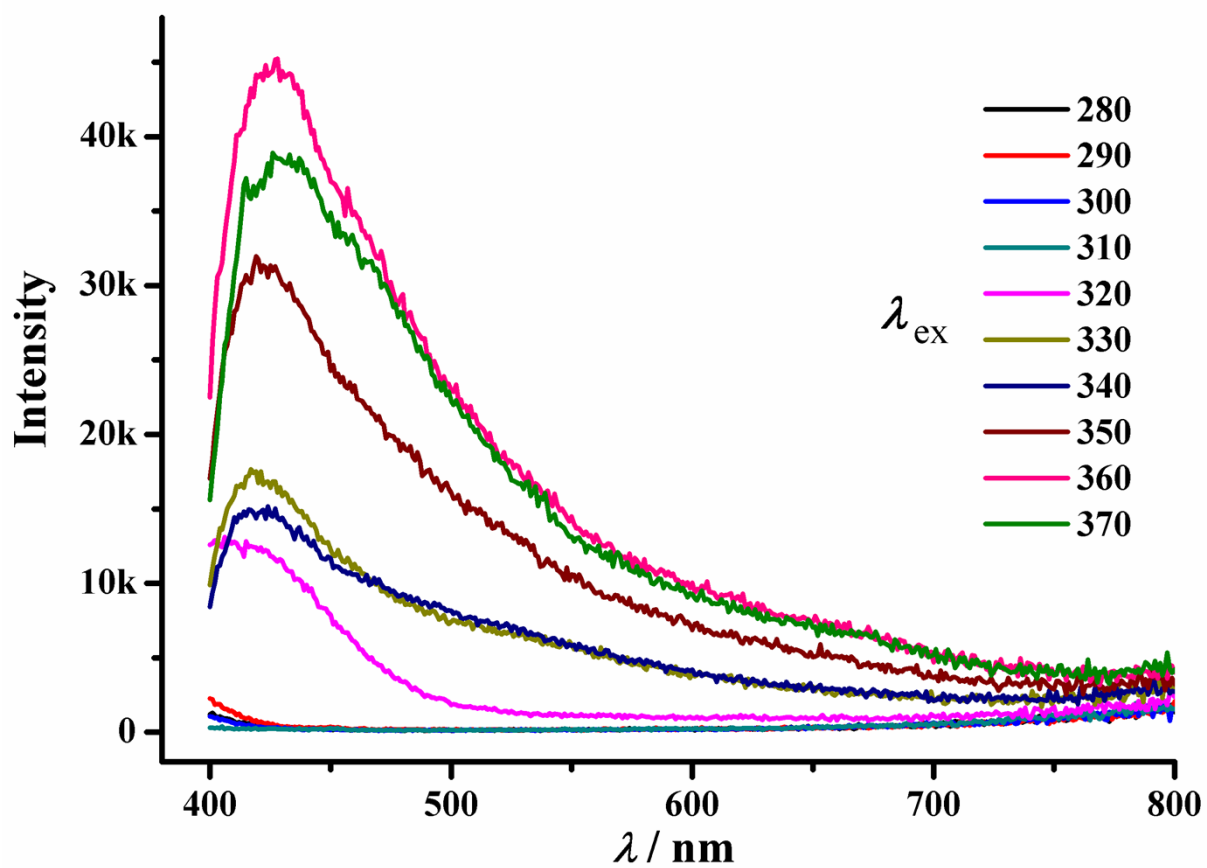


Fig. S26. The solid-state photoluminescence spectra of $(\text{Me}_2\text{DABCO})_2(\text{PbCl}_6)$.